

A Prediction Model for Formation Energy of Cobalt-Gold Nanoparticles Synthesis

Swami Nisha Bhagirath, Vaibhav Bhatnagar* and Linesh Raja

Department of Computer Applications, Manipal University Jaipur, India

*Correspondence to:

Vaibhav Bhatnagar
Department of Computer Applications,
Manipal University,
Jaipur, Rajasthan, India.
E-mail: vaibhav.bhatnagar15@gmail.com

Received: October 20, 2023

Accepted: December 21, 2023

Published: December 27, 2023

Citation: Bhagirath SN, Bhatnagar V, Raja L. 2023. A Prediction Model for Formation Energy of Cobalt-Gold Nanoparticles Synthesis. *NanoWorld J* 9(S5): S361-S366.

Copyright: © 2023 Bhagirath et al. This is an Open Access article distributed under the terms of the Creative Commons Attribution 4.0 International License (CCBY) (<http://creativecommons.org/licenses/by/4.0/>) which permits commercial use, including reproduction, adaptation, and distribution of the article provided the original author and source are credited.

Published by United Scientific Group

Abstract

The production of nanoparticles (NPs) is crucial to the development of nanotechnology, which has become well-known and has a wide range of uses. The size of a NPs can range from one to one hundred nanometers. Their physical and chemical features set them apart from their bulk equivalents, which makes them desirable for a range of cutting-edge applications. NPs made of a mixture of cobalt (Co) and gold (Au) components are referred to as cobalt-gold (Co-Au) NPs. Bimetallic Co-Au NPs have distinctive properties that make them particularly valuable in a variety of applications, including biological imaging and catalysis. Predictive models have gained popularity as a means of streamlining and improving NPs production procedures. In this paper, the prediction model is developed using Jamovi and orange data mining tool. The mean is 851.4560, the median is 553.2310 and the dispersion is 0.9058. According to the linear regression, R is 0.976, R² is 0.953, and adjusted R² is 0.953.

Keywords

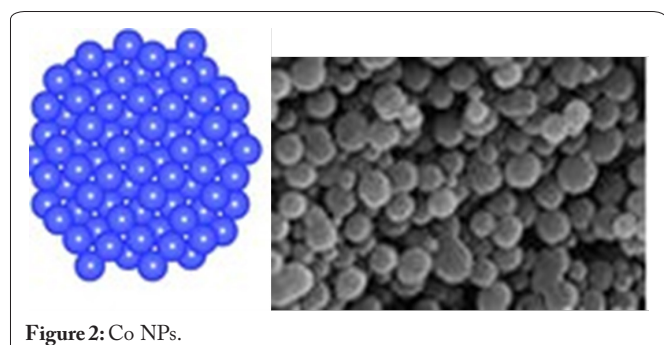
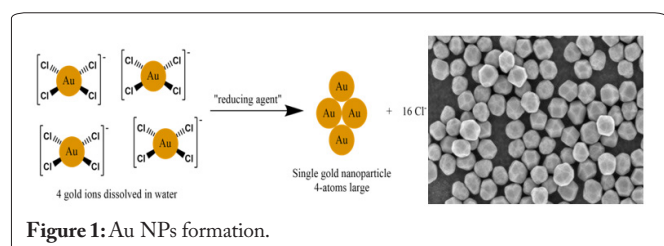
Cobalt-gold nanoparticles, Data mining, Regression, Nanoparticle

Introduction

In ancient Greek, the word “nano,” which means “dwarf,” denotes a reduction in size or duration by a factor of 10⁻⁹, or a billionth of a meter [1]. Utilizing tools and materials that can leverage substance molecular properties to explore the biological and material worlds at the nanoscale scale, nanotechnology is a relatively new research technique. As a result of their high sensitivity and real-time monitoring capabilities, nanosensors produce enormous volumes of data [2]. Techniques used in data science, such as data collecting, cleansing, preprocessing, and storage, make it possible to handle and organize this data effectively for analysis. Chemical engineering, chemistry, biochemistry, solid state physics, and materials science are all incorporated within nanotechnology [3]. The discipline of nanomedicine has emerged as a result of the revolutionary changes in biomedical research and healthcare applications brought about by the special features demonstrated by NPs and nanoscale materials [4]. Due to their small size and high surface area-to-volume ratio, NPs usually exhibit distinctive and improved characteristics in comparison to their bulk counterparts. These characteristics make NPs extremely appealing for a variety of applications across several fields [5]. The bimetallic nanomaterial known as Co-Au NPs is made of both Co and Au [6]. These NPs are appealing for a variety of applications, including the creation of nanosensors. Nanosensors are objects or substances that operate at the nanoscale and have a high sensitivity and selectivity for detecting and reacting to certain physical or chemical stimuli due to their distinctive features that result from the combination

of the two metals. The performance and scope of use of nanosensors can be improved by adding Co-Au NPs. Due to the interaction of their conduction electrons with light, Co-Au NPs display strong plasmonic characteristics [7]. Plasmonic nanosensors use these characteristics to detect analytes such as biomolecules, gases, and chemicals with extreme sensitivity and without the use of labels. Real-time sensing is made possible by alterations in the plasmon resonance peak brought on by changes in the local refractive index brought on by the binding of the analyte. The magnetic properties of the nanomaterial are provided by the cobalt in Co-Au NPs. Magnetic nanosensors can take advantage of this magnetic feature to detect specific targets or keep an eye on biological processes. Applications for Co-Au based biosensors include food safety, environmental monitoring, and medical diagnostics [8]. For bimetal NPs the use of Co is important. The Co NPs have remarkable magnetic, electrical and catalysis features that are beneficial in a selection of technological applications, with magnetic reminiscences, recording media, magnetic sensors, magnetic solutions, magnetic mixtures, magnetic reminiscences, and catalysis [9]. The formation of Au NPs is shown in figure 1 and Co NPs is shown in figure 2.

The Co NPs can be used for high-frequency circuits and wireless communications because they can absorb radiation. Because of their nano-size and unique physico-chemical characteristics, Co NPs are excellent sensors for a wide range of elements. The Au NPs absorb, scatter, and convert light energy into heat via surface chemistry and nonradioactive electron relaxation dynamics [10]. Due to their potential usage as drug carriers, they are desirable and adaptable NPs. The Au NPs are particularly sought-after in the biomedical industry due to their excellent stability and biocompatibility, simplicity in surface functionalization, low toxicity, and drug transferability. To make biosensors, Co-Au NPs can be functionalized with particular biomolecules. These biosensors are able to identify and bind to certain infections, disease related chemicals, or biomarkers, producing detectable signals.



The objectives of the studies were: (1) to provide a descriptive analysis of the Co-Au NPs dataset and (2) to implement linear regression model for formation energy of the Co-Au NPs.

In the literature, a number of similar approaches outlined in this study have been proposed. Milan et al. [11] and Sengupta et al. [12] suggested the prospective uses of Au NPs in the creation of fresh therapeutic and diagnostic approaches in nanomedicine, including their biological application as a drug carrier, as a component in radio and phototherapy, and in bio-imaging for image diagnostics. Ali et al. [13] analyzed an X-ray diffraction to determine the phase structure of the produced NPs. Utilizing UV-Vis spectroscopy and vibrating sample magnetometer techniques, the optical and magnetic properties of the generated materials are examined. The mutagenesis impacts of Au/Co NPs did not affect the *Salmonella typhimurium* TA-98 or TA-100 strains. Equipment created in the lab was used to look into the magnetic hyperthermia of Au/Co nanofluid. A specific absorption rate of 4.4 W/g for a magnetic field of 177 T was computed. Wang et al. [14] designated that the created multifunctional catalytic nanomaterial can be used as an excellent ECL (electro-chemiluminescent) signal reporter to increase the sensitivity of ECL biosensors through synergistic and zero-distance catalysis. A new catalytic nanomaterial called Co-MOF@AuNP@ABEI has been produced by mixing Co-doped metal-organic frameworks (Co-MOF), Au NPs, and N-(4-aminobutyl)-N-(ethylisoluminol). This nanomaterial enhances the sensitivity of an ECL biosensor through outstanding catalytic characteristics and synergistic effects. The Co-MOF@AuNP@ABEI nanomaterial provides an ultrasensitive detection of *Burkholderia pseudomallei* with an extraordinarily low limit of detection of 60.3 aM when combined with a 3D magnetic walking nanomachine amplification method. Al-Saif et al. [15] created a high level of accuracy artificial neural network model when assessing the chemical characteristics of fresh citrus fruit. High prediction and practicality of the model were provided by the relative errors acquired using the artificial neural network technique. The FD and FL variables in chemical attribute modeling showed good contribution ratios, leading to a trustworthy predictive model. MacKinnon et al. [16] created a progressive testing strategy to determine the ideal level of grouping. Simulations indicate that bootstrap tests have a lot of power and work well under the null hypothesis. An empirical example demonstrates that using the tests yields judgments that are reasonable.

Materials and Method

Data collection

Data collection is the process of acquiring pertinent and accurate information from a variety of sources for use in analysis, modeling, and decision making. The linear regression prediction model analysis is performed in Jamovi. Jamovi is an intuitive statistical tool that carries out a number of analyses, including linear regression. The dataset consists of a total of 4000 data. When predicting the properties of NPs, the performance of the linear regression model is measured using statistical metrics like mean squared error and R-squared. There are regions and sizes with both crystalline and non-

crystalline structures, ranging in size from 181 to 6083 atoms [17]. Several topological characteristics, such as size, lattice structure, surface curvature, and various order factors, have been used to characterize each NP. The final two columns, which contain target labels and the total energy and excess formation energy, are used to display the energy. In table 1, the parameters description of the Co-Au NPs is shown.

Data description

The mean and median are measures of central tendency in feature statistics, while measurements of dispersion reveal the distribution or variability of the data. The meaning is the mathematical average of a group of numbers. The median divides a sorted dataset into two equal halves by being the midpoint value. The median is frequently employed when a dataset has outliers or a skewed distribution since it is resistant to extreme values (outliers). In table 2, the feature statistics of the given dataset are shown.

Measures of dispersion, called measures of variability, describe how widely dispersed or variable a dataset is. They reveal how far the individual data points depart from the measurements of central tendency (mean or median). Metrics for dispersion shed light on the distribution and variability of the data points surrounding the central tendency. Basic statistics are employed to encapsulate and comprehend the properties of a dataset, including the mean, median, and measures of dispersion.

The prediction is performed in orange data mining tool. Orange is an open-source data analysis, data visualization, and machine learning application created. Orange is a Python program that is used extensively across many industries, including academia, research, and business. Orange offers a number of features for data preprocessing, such as handling missing values, feature scaling, normalization, feature selection, and more. These preprocessing procedures are essential for getting the data ready before creating models. The test and score are used for evaluation of the model. In figure 3, the linear regression model for Co-Au NPs dataset is shown. Linear regression is a key technique in the data scientist arsenal for tasks including prediction, inference, and detecting correlations within data. The use of linear regression allows data scientists to make inferences about the relationships between different variables. They are able to test hypotheses and determine whether a relationship between independent and dependent variables is statistically significant.

Results and Discussion

The output of a linear regression analysis contains a number of parameters and findings that shed light on the correlations between variables and the effectiveness of the fitted model. The dependent variable for the model is Formation_E which is formation energy of the atoms. Upper values, from range 0 to 1, represent a better fit to the data. In table 3, the results of model fit measures are shown. The linear regression gives R value as 0.976, R² value as 0.953 and adjusted R² value as 0.953. In table 4, the coefficients of the model are shown.

The differences between the observed values of the de-

Table 1: Co-Au NPs dataset parameters description.

S. No.	Labels	Description
1	ID	Unique identifier
2	T	Temperature, K
3	T_au	Total number of Au atoms
4	Time	Time
5	N_total	Number of total atoms
6	N_bulk	Number of total bulk atoms
7	N_surface	Number of total surface atoms
8	FCC	Total atoms in face centered cubic lattice
9	HCP	Total atoms in hexagonal closed packed lattice
10	ICOS	Total atoms in icosahedral lattice
11	DECA	Total atoms in decahedral lattice
12	Total_E	Total energy of the nanoparticle
13	Formation_E	Formation energy of the nanoparticle

Table 2: Feature statistics of given dataset.

S. No.	Labels	Mean	Median	Dispersion
1	ID	2000.50	2000.50	0.58
2	T	615	598	0.36
3	T_au	5.5e-05	0.00	1.4771
4	Time	8.20	10	0.35
5	N_total	3476.79	1867	1.06
6	N_bulk	2521.55	1199	1.18
7	N_surface	955.24	666	0.76
8	FCC	1002.64	326.50	1.65
9	HCP	190.10	20	2.41
10	ICOS	0.05	0	4.82
11	DECA	6.38	0	2.59
12	Total_E	-12472.6618	-6754.7829	-1.07428
13	Formation_E	851.4560	553.2310	0.9058

Table 3: Measures for model fit.

Model	R	R ²	Adjusted R ²
1	0.976	0.953	0.953

Table 4: Model coefficients - Formation_E.

Predictor	Estimate	SE	t	p
Intercept	-219.9860	14.41594	-15.260	<0.001
T	0.3977	0.01425	27.907	<0.001
Tau	-32011.8249	43334.37530	-0.739	0.460
Time	16.4630	1.22992	13.385	<0.001
FCC	-0.1129	0.00287	-39.298	<0.001
HCP	-0.5198	0.00893	-58.201	<0.001
ICOS	5.0307	11.38349	0.442	0.659
DECA	-0.9884	0.21427	-4.613	<0.001
Total_E	-0.0716	3.60e-4	-198.598	<0.001

pendent variable and those that the regression model anticipated are represented by residuals. Residuals offer important information regarding the precision and goodness of fit of the model predictions. In a linear regression analysis, the objective is to get the best-fitting line that minimizes the total of squared residuals. Residuals can be positive or negative. The

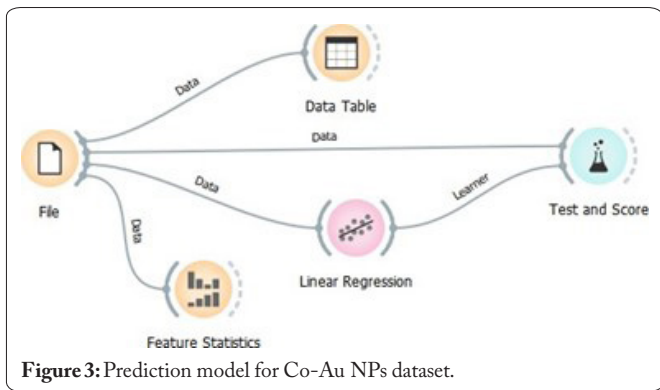


Figure 3: Prediction model for Co-Au NPs dataset.

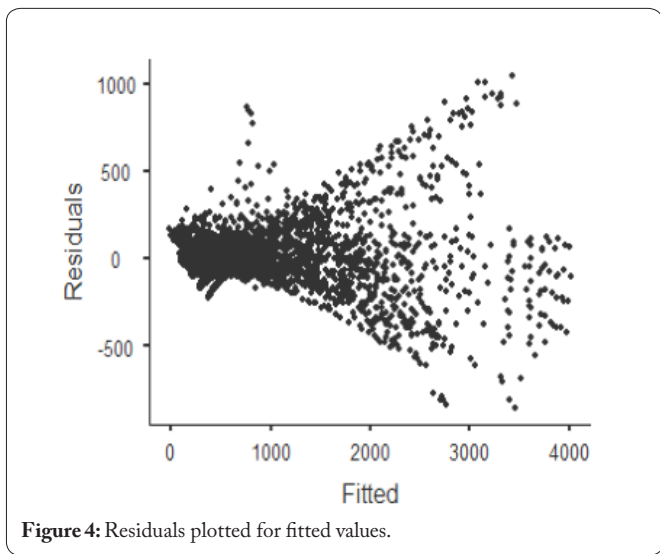


Figure 4: Residuals plotted for fitted values.

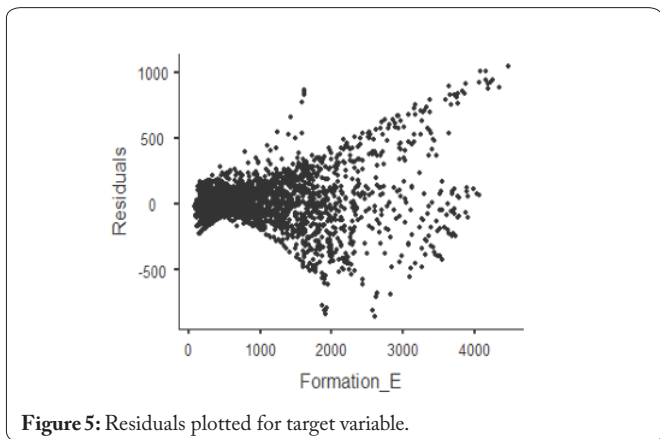


Figure 5: Residuals plotted for target variable.

following is how residuals are calculated as shown in equation 1.

$$\text{Residual} = \text{Observed Value} - \text{Predicted Value} \quad (1)$$

In figure 4, the residuals are plotted for fitted values. For target variable Formation_E, the residual is plotted in figure 5.

Figure 6, figure 7, and figure 8 show the residual plots of temperature, total number of Au atoms and time, respectively. Figure 9, figure 10, figure 11, and figure 12 show the residual plots of FCC, HCP, ICOS, and DECA, respectively. Similarly, figure 13 shows the residual plotting of total energy. For assessing the effectiveness of a linear regression model,

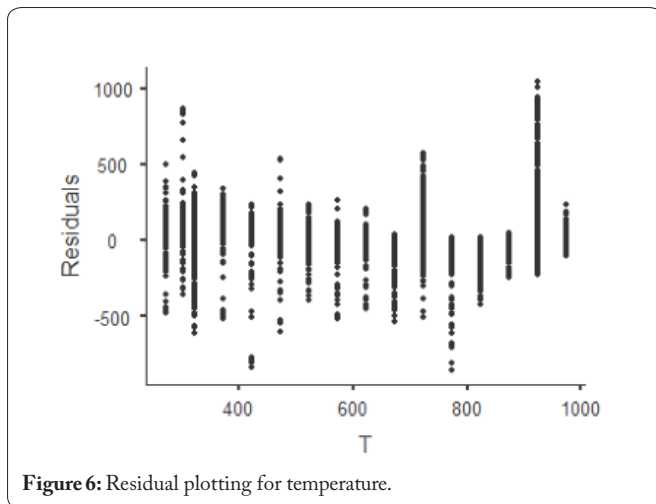


Figure 6: Residual plotting for temperature.

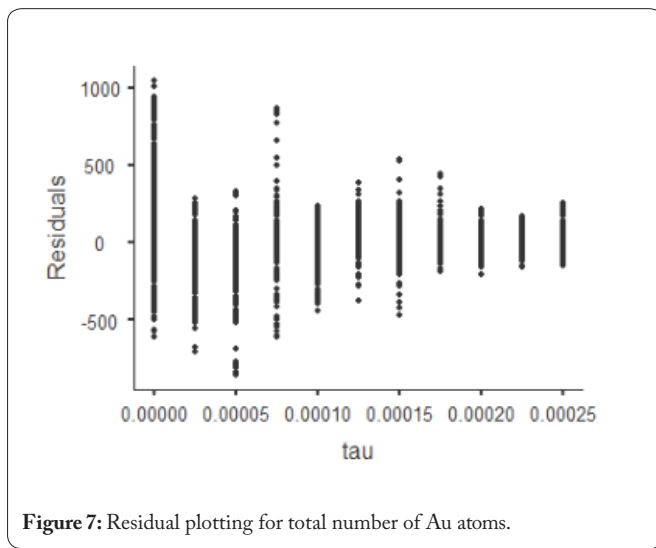


Figure 7: Residual plotting for total number of Au atoms.

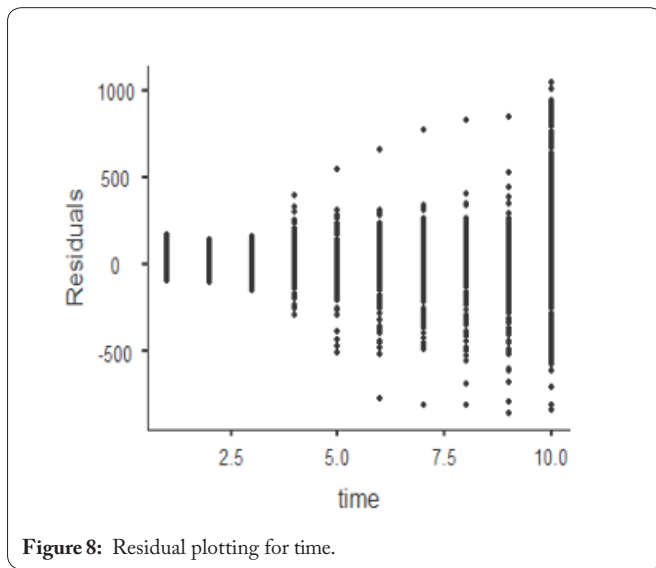


Figure 8: Residual plotting for time.

residuals are a vital tool. If the residuals are randomly distributed around zero and exhibit no discernible pattern, then the model assumptions are most likely correct, and the model fits the data well. Residuals can be used to identify outliers in the data. Outliers are data points with large residuals, which de-

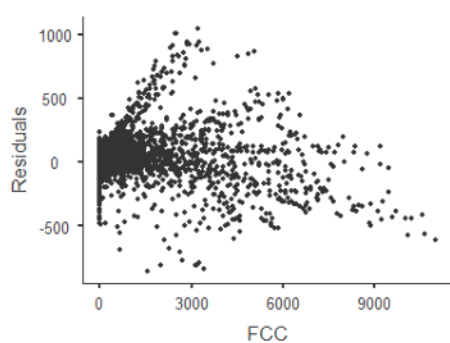


Figure 9: Residual plotting for number of atoms in FCC.

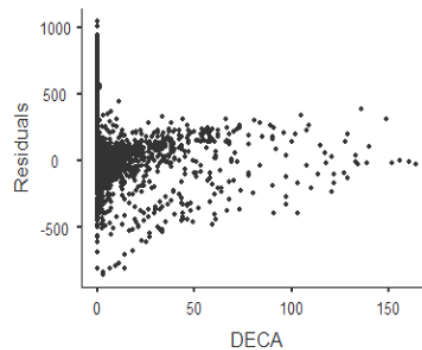


Figure 12: Residual plotting for number of atoms in DECA.

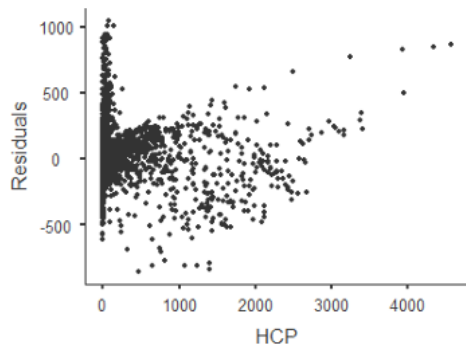


Figure 10: Residual plotting for number of atoms in HCP.

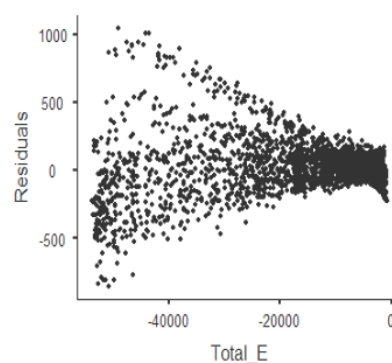


Figure 13: Residual plotting for total energy.

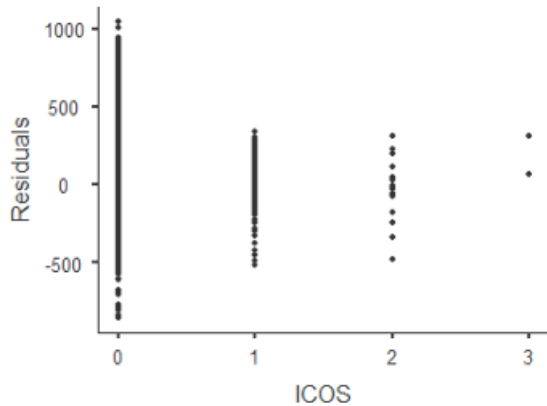


Figure 11: Residual plotting for number of atoms in ICOS.

note a considerable divergence from the anticipated values. The fit and result of the regression model may be significantly impacted by these abnormalities. Residual plots are visual representations where the anticipated values are shown on the X-axis and the residuals are shown on the Y-axis.

Conclusion

The effective use of data mining methods, particularly linear regression, to forecast the features of Co-Au NPs represents a significant advancement in the field of customized NP design. The prediction model is developed using Jamovi and orange

data mining tool in this paper. The mean is 851.4560, the median is 553.2310 and the dispersion is 0.9058. The linear regression gives R value as 0.976, R-squared value as 0.953 and adjusted R-squared value as 0.953. These method quantitative relationships enable researchers to improve nanoparticle performance, optimize synthesis conditions, and realize their full potential in catalysis, electronics, and medicine. The linear regression model provides a powerful approach to show measurable relationships between synthesis parameters and NPs characteristics.

Acknowledgements

None.

Conflict of Interest

The authors declare that they have no competing interests.

References

1. Fagundes AP, da Silva AH, Macuvele DL, Riella HG, Padoin N, et al. 2022. Plant-mediated Synthesis of Nanoscale Hydroxyapatite: Morphology Variability and Biomedical Applications. In Shanker U, Hussain CM, Rani M (eds) Handbook of Green and Sustainable Nanotechnology. Springer, Cham, pp 1-26.
2. McNeil SE. 2005. Nanotechnology for the biologist. *J Leukoc Biol* 78(3): 585-594. <https://doi.org/10.1189/jlb.0205074>
3. Bhattacharya T, Soares GA, Chopra H, Rahman MM, Hasan Z, et al. 2022. Applications of phyto-nanotechnology for the treatment of neurodegenerative disorders. *Materials* 15(3): 804. <https://doi.org/10.3390/ma15030804>

4. Zain M, Yasmeen H, Yadav SS, Amir S, Bilal M, et al. 2022. Applications of Nanotechnology in Biological Systems and Medicine. In Denizli A, Nguyen TA, Rajan M, Alam MF, Rahman K (eds) Nanotechnology for Hematology, Blood Transfusion, and Artificial Blood. Elsevier, pp 215-235.
5. Denizli A, Nguyen TA, Mariappan R, Alam MF, Rahman K. 2021. Nanotechnology for Hematology, Blood Transfusion, and Artificial Blood. Elsevier.
6. Hasan S. 2015. A review on nanoparticles: their synthesis and types. *Res J Recent Sci* 4: 9-11.
7. Cheng G, Walker AR. 2007. Synthesis and characterization of cobalt/gold bimetallic nanoparticles. *J Magn Magn Mater* 311(1): 31-35. <https://doi.org/10.1016/j.jmmm.2006.11.164>
8. Njuguna J, Pielichowski K, Zhu H, 2021. Health and Environmental Safety of Nanomaterials: Polymer Nanocomposites and Other Materials Containing Nanoparticles. Woodhead Publishing.
9. Satija J, Bharadwaj R, Sai VV, Mukherji S. 2010. Emerging use of nanostructure films containing capped gold nanoparticles in biosensors. *Nanotechnol Sci Appl* 3: 171-188. <https://doi.org/10.2147/NSA.S8981>
10. Ali H, Yadav YK, Ali D, Kumar G, Alarifi S. 2023. Biosynthesis and characterization of cobalt nanoparticles using combination of different plants and their antimicrobial activity. *Biosci Rep* 43(7): BSR20230151. <https://doi.org/10.1042/BSR20230151>
11. Milan J, Niemczyk K, Kus-Liškiewicz M. 2022. Treasure on the Earth—gold nanoparticles and their biomedical applications. *Materials* 15(9): 3355. <https://doi.org/10.3390/ma15093355>
12. Sengupta A, Azharuddin M, Al-Otaibi N, Hinkula J. 2022. Efficacy and immune response elicited by gold nanoparticle-based nanovaccines against infectious diseases. *Vaccines* 10(4): 505. <https://doi.org/10.3390/vaccines10040505>
13. Ali I, Pan Y, Jamil Y, Chen J, Shah AA, et al. 2023. Hybrid Au/Co nanoparticles: laser-assisted synthesis and applications in magnetic hyperthermia. *Phys B Condens Matter* 657: 414773. <https://doi.org/10.1016/j.physb.2023.414773>
14. Wang Y, Chen R, Shen B, Li C, Chen J, et al. 2022. Electrochemiluminescent (ECL) biosensor for *Burkholderia pseudomallei* based on cobalt-doped MOF decorated with gold nanoparticles and N-(4-aminobutyl)-N-(ethylisoluminol). *Microchim Acta* 189: 355. <https://doi.org/10.1007/s00604-022-05402-6>
15. Al-Saif AM, Abdel-Sattar M, Eshra DH, Sas-Paszt L, Mattar MA. 2022. Predicting the chemical attributes of fresh citrus fruits using artificial neural network and linear regression models. *Horticulturae* 8(11): 1016. <https://doi.org/10.3390/horticulturae8111016>
16. MacKinnon JG, Nielsen MØ, Webb MD. 2023. Testing for the appropriate level of clustering in linear regression models. *J Econom* 235(2): 2027-2056. <https://doi.org/10.1016/j.jeconom.2023.03.005>
17. Ting J, Barnard A, Opletal G. 2023. CoAu nanoparticle data set. *CSIRO*. <https://doi.org/10.25919/991j-hg07>